Conductivity of nanosecond discharges in nitrogen and sulfur hexafluoride studied by particle-in-cell simulations

D. Levko, V. Tz. Gurovich, and Ya. E. Krasik
Department of Physics, Technion, 32000 Haifa, Israel

(Received 23 April 2012; accepted 17 May 2012; published online 22 June 2012)

The conductivity of the discharge gap during the nanosecond high-voltage pulsed discharge in nitrogen and sulfur hexafluoride is studied using particle-in-cell numerical simulations. It is shown that the conductivity in different locations of the cathode-anode gap is not uniform and that the conductivity is determined by both the runaway and the plasma electrons. In addition, it is shown that runaway electrons generated prior to the virtual cathode formation pre-ionize the discharge gap, which makes it conductive. © *2012 American Institute of Physics*. [http://dx.doi.org/10.1063/1.4730373]

I. INTRODUCTION

Today, nanosecond high-voltage (HV) pulsed discharges in pressurized gases are applied in various areas, namely, plasma-assisted combustion,[1,2] pulsed gaseous lasers,[3] generation of electron beams and x-rays,[4–7] etc. The study of such discharges is of fundamental interest because the duration of the discharge is comparable with the duration of electron avalanching and decay time of the excited atoms and molecules. It is known[4–7] that the nanosecond discharges induced by large over-voltage are determined by the propagation of runaway electrons (RAE) toward the anode. These RAE are generated either in the vicinity of the cathode or in the volume of discharge in the non-uniform electric field typical for this type of discharge.

In order to increase the efficiency of the use of nanosecond discharge, one has to know the dependence of the conductivity of the discharge gap on the external parameters, such as gas pressure, amplitude of the cathode voltage, its rise time, and the cathode-anode (CA) gap. Akhmadeev *et al.*[8] studied experimentally the spark breakdown of air at atmospheric pressure using a pulsed GIN generator, the output of which was nanosecond pulses with a voltage amplitude of 18 kV and rise times of 8 ns and 30 ns. It was found that the CA gap impedance decreases during the discharge, reaching an almost constant value of tens of Ohms at its end.

Babich reported[9] that the conductivity of the nanosecond discharge at high over-voltages is controlled by both runaway and plasma electrons that are formed by the gas ionization and by the pre-ionization of the gas by anomalous electrons whose energy at the anode exceeds the energy that these electrons can gain at a given CA accelerating voltage. Babich concluded that the CA gap conductivity depends on the experimental conditions, namely, electric field distribution and the CA gap voltage. However, a detailed study of the influence of these parameters on the conductivity was not carried out.

This paper presents the results of a numerical study of the conductivity of nanosecond high-voltage discharge in nitrogen (N_2) and sulfur hexafluoride (SF_6) gases in various conditions.

II. NUMERICAL MODEL

In order to study the processes accompanying the nanosecond discharge, one-dimensional particle-in-cell (1D PIC) simulations, described in detail in Ref. 10, were used. A coaxial diode filled with either N_2 or SF_6 at pressures of 10^5 Pa and 2×10^5 Pa and with a cathode and anode radius of 3 μm and 1 cm, respectively, and a length of 1 cm was considered. Briefly, the sequence of 1D PIC simulation was as follows. (a) Solution of the Poisson equation at the beginning of each time step for new electron and ion space charge densities and for new boundary conditions; the anode is grounded and the cathode potential is varying in time as $\varphi_c = -\varphi_0 \sin(2\pi \cdot t/T)$, where $\varphi_0 = 120$ kV is the maximal cathode potential and $T/2$ is the HV pulse temporal duration. (b) Calculation of the number of emitted electrons defined by the field emission (FE) determined by the Fowler-Nordheim law.[11] (c) Solution of propagation equations for electrons and ions. (d) Electron elastic and inelastic collisions using the Monte Carlo methods, taking into account forward and backward scattering of electrons;[12] ionization and excitation of the electron levels $A^3\Sigma_u^+$ and $C^3\Pi_u$ [further denoted as $N_2(A)$ and $N_2(C)$, respectively] were considered for N_2, and ionization, excitation of the first electronic level, and attachment of electrons to molecules were considered for SF_6. (e) Particles weighting on the spatial grid and returning to step (a). The time step of 10^{-14} s allows us to consider electrons propagating only a part of the mean free path during one time step.

The dependencies of the conductivity and resistance at different distances from the cathode and time were calculated as

$$\sigma(r,t) = \frac{e}{2\pi \cdot l \cdot dt} \frac{dN_e(r,t)}{r\,E(r,t)} \text{ and } R(r,t) = \frac{1}{\sigma(r,t)} \frac{dr}{2\pi \cdot rl}, \quad (1)$$

respectively. Here e is the electron charge, dt is the time step, l is the cathode length equal to 1 cm, r is the distance with respect to the cathode, $E(r,t)$ is the electric field at the distance r at given time, $dN_e(r,t)$ is the number of electrons that have passed the distance r towards the anode, and dr is the space step.

III. RESULTS AND DISCUSSION

In a previous study,[10] it was shown that in the cathode vicinity, where one obtains a highly non-uniform electric

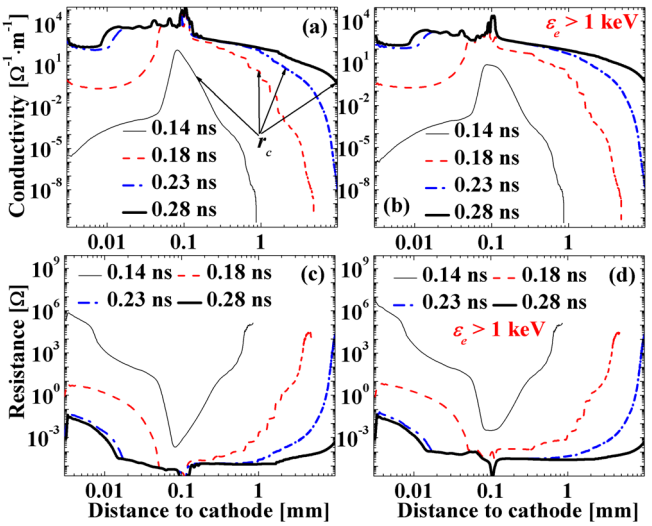

FIG. 1. (a) and (b) Dependence of the conductivity and (c) and (d) resistivity on the distance to the cathode at different times of the accelerating pulse; $T/2 = 1$ ns, $\varphi_0 = 120$ kV, $P = 10^5$ Pa, N_2 gas.

field, the separation between electrons and ions causes formation of the virtual cathode (VC), which influences significantly the discharge dynamics. Namely, on the one hand, the VC terminates the RAE formation from the field-emitted electrons and plasma electrons in the vicinity of the cathode. On the other hand, the VC can be considered as the source of RAE if the electric field from its anode side exceeds the critical electric field E_{cr} required for RAE generation (for instance, $E_{cr} = 4.5 \times 10^5$ V/cm in nitrogen at atmospheric pressure). Thus, the dynamics of the VC evolution influences the conductivity of the CA gap during the nanosecond discharge. For instance, at accelerating pulse with duration of $T/2 = 1$ ns, $P = 10^5$ Pa, and $\varphi_0 = 120$ kV, the VC is already formed in nitrogen at $t_{VC} \approx 0.22$ ns.

Figs. 1(a) and 1(b) and Figs. 1(c) and 1(d) show the dependencies of conductivity and resistance, respectively, on the distance to the cathode at different time delays τ_d with respect to the beginning of the accelerating pulse. Here, in Figs. 1(a) and 1(c), the conductivity and resistance are defined by electrons with all energies, whereas in Figs. 1(b) and 1(d), the conductivity and resistivity are defined only by the electrons that have energies $\varepsilon_e > 1$ keV and are considered as RAE. One can see that both the conductivity and resistance of the CA gap are not spatially uniform reaching maximum and minimal values, respectively, at locations where the maximum plasma density [see Fig. 2(b)] is formed. The conductivity increases sharply from zero value at the front of the RAE propagating towards the anode. In addition, it was obtained that at a distance larger than some value $r > r_C$ [see Fig. 1(a)] the conductivity of the discharge gap is defined only by RAE, and at distances $r < r_C$, the conductivity is defined by both RAE and the plasma electrons.

The boundary of the plasma r_c, which separates the regions of conductivity that are defined only by RAE and the plasma electrons together with RAE, propagates toward the anode with an average velocity of ~ 2 cm/ns. This value is in rather good agreement with the velocity of the light emission front obtained by Yatom *et al.*[13] Indeed, Fig. 2(a) shows the simulated dependence of the number of electronically excited $N_2(C)$ on the distance to the cathode at different values of τ_d. One can see that the boundary of excited $N_2(C)$ propagating toward the anode coincides with the boundary r_c, separating the region where the conductivity is defined only by RAE that cannot excite the nitrogen effectively because of small cross sections.[12] However, RAE pre-ionize the discharge gap,[10,14] which leads to an increase in the conductivity behind their propagating front. Electrons that are generated by RAE gain energy in the electric field, which is much smaller than the electric field in the vicinity of the cathode (for instance, at $t \approx 0.13$ ns, the electric field at the cathode is $\approx 2 \times 10^7$ V/cm and at $r = 0.1$ mm is $\approx 6.5 \times 10^5$ V/cm). Therefore, the rate of energy gain by these electrons is lower and these electrons excite nitrogen effectively due to larger excitation cross-section. The latter results in the propagation of a light emission front with a high velocity.

Fig. 2(b) shows the density of plasma electrons ($\varepsilon_e \leq 30$ eV) versus the distance to the cathode at different values of τ_d. One can see that the location of the maximum values of conductivity [see Fig. 1(a)] and $N_2(C)$ density [see Fig. 2(a)] coincides with the location of maximum electron density, which reaches $\sim 10^{16}$ cm^{-3}. Taking into account that the gas density is $\sim 2.6 \times 10^{19}$ cm^{-3}, one can conclude that the degree of gas ionization does not exceed $\sim 10^{-3}$, which allows one to define this gas as a low-ionized plasma in which resistivity is governed by electron-neutrals collisions. Fig. 2(c) shows the time evolution of the potential difference φ between the cathode and cross-sections located at distances of 0.1 mm $\varphi(0.1\text{ mm})$ and 1 mm $\varphi(1\text{ mm})$. These potential differences were calculated as $\sum_{i=1}^{N} R_i I_i$, where N is the number of space cells between the cathode and given cross-section. These cells were considered as conductors with the resistance of each cell R_i and the current I_i which flows through this cell. The value of the current I_i is proportional to dN_e, while the value of the resistance is proportional to $E(r,t)/dN_e$ [see Eq. (1)]. Therefore, the potential difference

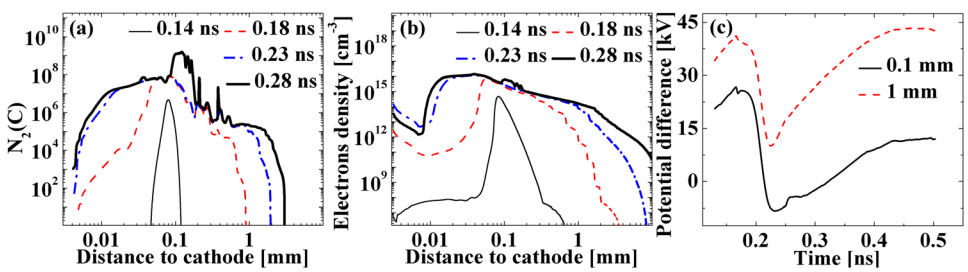

FIG. 2. Dependence of the number of excited $N_2(C)$ (a) and of the plasma electrons density (b) on the distance to the cathode at various times of the accelerating pulse; (c) time dependence of the potential difference between the cathode and cross-sections placed at 0.1 mm and from the cathode; $T/2 = 1$ ns, $\varphi_0 = 120$ kV, $P = 10^5$ Pa, N_2 gas.

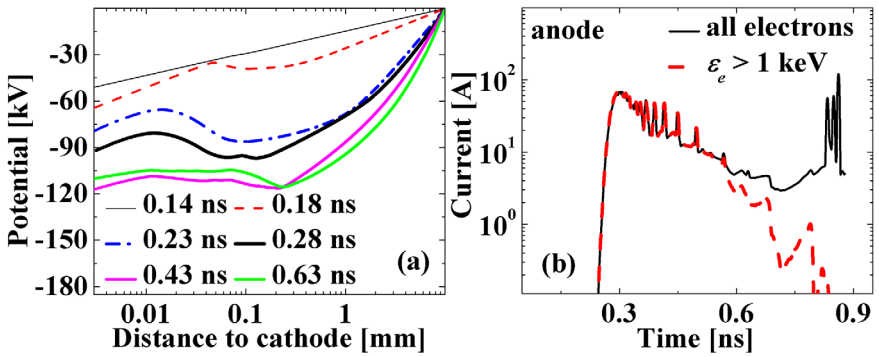

FIG. 3. (a) Potential distribution in the CA gap at different times of accelerating pulse; (b) time dependence of the number of electrons with all energies and with energies exceeding 1 keV passing through the anode; $T/2 = 1$ ns, $\varphi_0 = 120$ kV, $P = 10^5$ Pa, N_2 gas.

for a given cell is proportional only to the electric field $E(r,t)$ in that cell. The increase in value of φ at $0 < \tau_d < 0.17$ ns is caused only by the increase of the cathode potential and of $E(r,t)$, respectively, since the space charge of the emitted electrons and generated plasma particles does not influence significantly the potential distribution at that time. Later the space charge increases significantly [see Fig. 2(b)] and starts to disturb external electric field that causes a decrease of the potential difference. Fig. 2(c) shows that at $\tau_d \approx t_{VC}$ the value of $\varphi(0.1\,\text{mm}) = \varphi_c$ what indicates the high-conductivity plasma channel formation at the distance $r < 0.1$ mm. At time $\tau_d > t_{VC}$ one obtains $|\varphi(0.1\,\text{mm})| > |\varphi_c|$ due to accumulation of electrons at the VC location. When the VC becomes the source of RAE and it starts to move towards the anode one obtains the increase of $\varphi(0.1\,\text{mm}) - \varphi_c$. Also, Fig. 2(c) shows that at $r = 1$ mm the value of $|\varphi(1\,\text{mm})| < |\varphi_c|$ because the VC does not reach that location. These results indicate that the region of high-conductivity plasma exists only in the limited space $r \leq 0.3$ mm [see Fig. 3(a)].

Fig. 3(a) shows that the VC, which is formed $r_{VC} < 0.1$ mm at $t_{VC} \approx 0.22$ ns, propagates towards the anode. The formation and propagation of the VC influences significantly the total current through the CA gap. Fig. 3(b) shows that at $\tau_d < 0.63$ ns the current through the anode is defined by the RAE generated prior to the VC formation since the plasma electrons do not shift noticeably toward the anode at the considered time scale. Later, when the RAE generation is terminated, the current is defined by plasma electrons which determine the conductivity at that time.

In order to compare the conductivity in different gases, additional simulations were carried out for SF_6 gas. The ionization potentials of SF_6 ($\approx$16 eV) and N_2 ($\approx$15.6 eV) do not differ significantly. However, the ionization cross section σ_{ion} for SF_6 is larger than for N_2. For example, in SF_6, the largest value of $\sigma_{ion} \approx 7.6 \times 10^{-16}$ cm^2, while in N_2 it is $\sigma_{ion} \approx 2.6 \times 10^{-16}$ cm^2, i.e., in the case of equal electron temperature, the rate of ionization in SF_6 is larger than in N_2. In addition, SF_6 gas has an additional source of inelastic losses of electron energy: the electrons' attachment to neutrals. This process decreases significantly the number of low-energy electrons and increases the time of the gas gap breakdown with dense plasma formation, respectively (see Ref. 15).

Fig. 4 shows the time dependence of the total resistance of the discharge gap defined by electrons with all energies and electrons, with $\varepsilon_e > 1$ keV in N_2 and SF_6 gases. As one can expect, the resistance decreases from infinity, when RAE do not reach the anode, to some constant value. The simulation results showed that at $T/2 = 1$ ns, $\varphi_0 = 120$ kV, and $P = 10^5$ Pa, the resistance in the case of N_2 is $\sim$1 Ω, larger than for the case of SF_6 gas where it is $\sim$0.5 Ω. In addition, one can see that the resistance of the discharge gap filled with SF_6 decreases faster than the resistance of the gap filled with N_2. This result disagrees with the experimental data presented in Ref. 16 where the resistance of the discharge channel formed in the SF_6 was found to be larger than the resistance of the discharge channel formed in N_2. Here the resistance was calculated using the measured accelerating voltage and the current of electrons penetrating through the anode foil. Thus, the apparent disagreement between the experimental and simulation results can be explained by the cutoff of low-energy electrons propagating through the anode foil. Considering Eq. (1), one can conclude that the resistance of discharge channel is proportional to $E(r,t)/(dN_e/dt)$. However, the ionization cross-section for the same electron temperature is larger for SF_6 than for N_2. The latter leads to larger value of dN_e/dt in SF_6 than in N_2, and therefore, for the same electric field one obtains larger resistance of the plasma channel for N_2 than for SF_6. It is important to note that the rate of electron attachment to SF_6 does not exceed the rate of ionization.

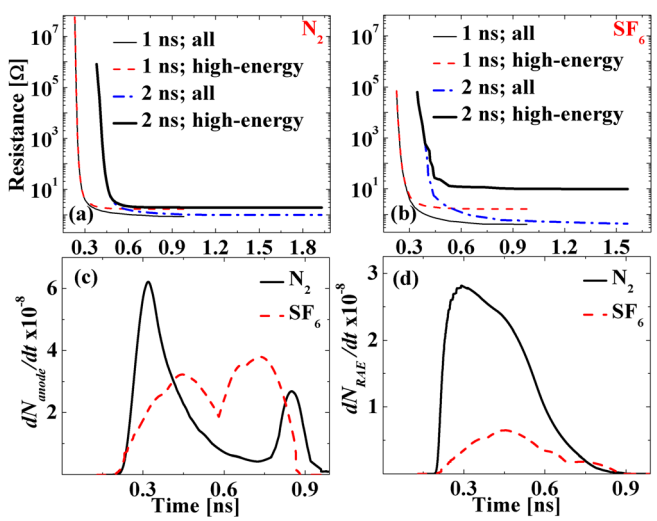

FIG. 4. Time dependence of the total resistivity of discharge gap filled with N_2 (a) and SF_6 (b) gases; (c) the total number of electrons crossing the anode per time step; (d) the number of RAE crossing the anode per time step.

TABLE I. The distribution of energy among various channels in N_2.

N_2	Beam at the anode	Electrons in CA gap	Ionization	N_2 (A)	N_2 (C)
10^5 Pa, 1 ns	1.6×10^{-4} J (36.9%)	3.7×10^{-6} J (0.9%)	2.6×10^{-4} J (61.2%)	1.9×10^{-6} J (0.4%)	2.7×10^{-6} J (0.6%)
2×10^5 Pa, 1 ns	2.2×10^{-5} J (13.6%)	1×10^{-5} J (6.2%)	1.3×10^{-4} J (79.5%)	4×10^{-7} J (0.2%)	7.4×10^{-7} J (0.5%)
10^5 Pa, 2 ns	1.5×10^{-4} J (38.1%)	4×10^{-6} J (1.0%)	2.4×10^{-4} J (59.7%)	2.5×10^{-6} J (0.6%)	2.5×10^{-6} J (0.6%)

TABLE II. The distribution of energy among various channels in SF_6.

SF_6	Beam at the anode	Electrons in CA gap	Ionization	Excitation
10^5 Pa, 1 ns	1.6×10^{-5} J (2.9%)	6.7×10^{-8} J (0.01%)	5.3×10^{-4} J (96.0%)	5×10^{-6} J (1.1%)
2×10^5 Pa, 1 ns	2.9×10^{-6} J (0.8%)	6.8×10^{-6} J (1.8%)	1.1×10^{-3} J (96.9%)	5.3×10^{-6} J (0.5%)
10^5 Pa, 2 ns	6.5×10^{-6} J (1.0%)	1.8×10^{-7} J (0.1%)	5.9×10^{-4} J (98.0%)	5.3×10^{-6} J (0.9%)

Therefore, fast decay of the plasma does not start at the considered time scale.

The comparison between the total number of electrons dN_{anode}/dt and the number of RAE dN_{RAE}/dt crossing the anode during each time step in N_2 and SF_6 gases is shown in Figs. 4(c) and 4(d), respectively. One can see that the total number of electrons crossing the anode in SF_6 is larger than that in N_2 at time $0.4\,\text{ns} < t < 0.85\,\text{ns}$ in spite of excess of the number of RAE generated in N_2. Thus, this result also indicates the smaller resistance of the discharge gap filled with SF_6.

In addition, it was obtained that the increase in the gas pressure up to 2×10^5 Pa increases the resistance up to $\sim 1.6\ \Omega$ and $\sim 1.3\ \Omega$ in the cases of N_2 and SF_6, respectively. Also, in both gases, the increase in the voltage rise time increases slightly the resistance defined by all electrons, and in the case of SF_6, this increase in the resistance is defined by RAE.

Tables I and II show the distribution of energy among various channels in the case of discharges in N_2 and SF_6 gases. Depending on the application (laser pumping, plasma assisted combustion, electron beam generation, etc.), these energy channels could be considered either profitable or non-profitable. One can see that in both the gases the ionization process is the main channel of energy deposition. However, in the same conditions in the case of the discharge in N_2 gas, more than 30% of energy goes into the generation of the electron beam that reaches the anode, whereas in the case of the discharge in SF_6 gas, this energy does not exceed 3%.

IV. SUMMARY

To conclude, the results of 1D PIC simulations of the conductivity of the discharge gap during the nanosecond discharge in N_2 and SF_6 gases are presented. It was obtained that the conductivity is not uniformly distributed in the accelerating gap and that the conductivity of the discharge cannel is defined by RAE or by both the RAE and plasma electrons. In addition, it is shown that RAE generated prior to the virtual cathode formation pre-ionize the discharge gap, which makes it conductive.

ACKNOWLEDGMENTS

This work was supported in part at the Technion by a fellowship from the Lady Davis Foundation.

[1]S. M. Starikovskaya, J. Phys. D: Appl. Phys. **39**, R265 (2006).
[2]S. A. Bozhenkov, S. M. Starikovskaia, and A. Yu. Starikovskii, Combust. Flame **133**, 133 (2003).
[3]G. A. Mesyats, V. V. Osipov, and V. F. Tarasenko, *Pulsed Gas Laser* (SPIE, Bellingham, WA, 1995).
[4]L. P. Babich, T. V. Loiko, and V. A. Tsukerman, Phys. Usp. **33**, 521 (1990).
[5]A. V. Gurevich and K. P. Zubin, Phys. Usp. **44**, 1119 (2001).
[6]V. F. Tarasenko and S. I. Yakovlenko, Phys. Usp. **47**, 887 (2004).
[7]V. F. Tarasenko, E. K. Baksht, A. G. Burachenko, I. D. Kostyrya, M. I. Lomaev, and D. V. Rybka, Plasma Devices Oper. **16**, 267 (2008).
[8]V. V. Akhmadeev, L. M. Vasylyak, S. V. Kostyuchenko, N. N. Kudryavtsev, and G. A. Kurkin, J. Tech. Phys. **66**, 58 (1996), available at http://journals.ioffe.ru/jtf/1996/04/page-58.html.ru (in Russian).
[9]L. P. Babich, *High-Energy Phenomena in Electric Discharges* (Futurepast, Arlington, VA, 2003).
[10]D. Levko, S. Yatom, V. Vekselman, J. Z. Gleizer, V. Tz. Gurovich, and Ya. E. Krasik, J. Appl. Phys. **111**, 013303 (2012).
[11]Yu. P. Raizer, *Gas Discharge Physics* (Springer, Berlin, 1991).
[12]Y. Itikawa, J. Phys. Chem. Ref. Data **35**, 31 (2006).
[13]S. Yatom, V. Vekselman, J. Z. Gleizer, and Ya. E. Krasik, J. Appl. Phys. **109**, 073312 (2011).
[14]D. Levko, V. Tz. Gurovich, and Ya. E. Krasik, J. Appl. Phys. **111**, 013306 (2012).
[15]D. Levko and Ya. E. Krasik, J. Appl. Phys. **111**, 013305 (2012).
[16]E. H. Baksht, A. G. Burachenko, I. D. Kostyrya, M. I. Lomaev, D. V. Rybka, M. A. Shulepov, and V. F. Tarasenko, J. Phys. D: Appl. Phys. **42**, 185201 (2009).